Chapter 5

System Simulation

5.1 Introduction

A mathematical model, which consists of a set of equations, for predicting the system thermal performance of the designed built-in-storage solar water heater has been developed in Chapter 3. Several experimental tests on the constructed built-in-storage solar water heater have also been carried out and the results obtained have already been presented in Chapter 4. In this chapter, verification of the thermal performance of the solar water heater simulated by the developed model was investigated. In the investigation, a simulation program was constructed based on the model developed in Chapter 3. The program was written using Visual Basic version 6 compiler. The simulation results were verified in comparison with the experimental results obtained in Chapter 4.

5.2 System Simulation Procedure

As mentioned in Chapter 3, a finite difference method has been used to solve the thermal performance of the constructed BIS system by dividing the system into several portions along the length of the system as shown in Fig. 3.3. For the simulation the BIS system was divided into 17 portions along the length of the collector. Since the measurement points of the water temperatures in the BIS system were located at both ends of the collector (about 50 mm from the side wall) and at the middle of the collector length. Therefore it can be found that portions 1, 9, and 17 of the simulation system are approximately at the measurement points fixed in the experimental system. The reason for this arrangement is that the simulation results can be compared with those obtained from the experiment.

Figure 5.1 shows the flow chart of system simulation procedure of the designed built-in-storage solar water heating system. The simulation starts with the setting up of various known constant parameters: those are the tilt angle (θ), the latitude (Lat), the

collector width (B), the collector length (L), the collector channel depth (d), the insulation thickness (l_{os}), the heat conductivity of the insulation (k), the number of glass cover (N), the transmittivity of glass cover (τ_g),the emittivity of glass cover (ε_g), the emittivity of the absorber plate (ε_p), the absorbtivity of the absorber (α_p), the tank capacity ($\forall_s$), and the initial temperatures of water in the channel and the tank. Next the input file of the measured meteorological data, i.e. total solar radiation I_T, ambient temperature T_a, and wind speed v_{wind} are put in the simulation program. The number of time period desired for simulation is then entered. After this the program starts to determine the overall top loss coefficient U_{t_j} using eq. (3.4), the heat transfer coefficient between water in the collector channel the storage tank U_{sf} (i.e. k_{sf}/l_{sf}), a heat loss coefficient between the storage tank and ambient U_{os} (i.e. k_{os}/l_{os}). Next the convective heat transfer coefficient between the absorber and water in the collector channel h_f and the plate temperature T_p are calculated by eqs. (3.5) and (3.2) respectively. The thermosyphon head H_T and the thermosyphon mass flow rate $\dot{m}$ are calculated by eqs. (3.12) and (3.15) respectively. The temperature of water in the channel, $T_{f_j}^{t+\Delta t}$, and in the storage tank, $T_{s_j}^{t+\Delta t}$, are then calculated by eqs. (3.8) and (3.10) respectively. The values of H_T, $\dot{m}$, $T_{f_j}^{t+\Delta t}$ and $T_{s_j}^{t+\Delta t}$ are stored in an output data file. The simulation will continue until the number of time period is exceeded. Afterwards, the data stored in the output file are retrieved for further determinations of important parameters for indicating the system thermal performance. These parameters include the average temperatures at any time t of the water in the collector channel, T_{fm}^{t}, and in the storage tank, T_{sm}^{t}, the daily system useful energy, Q_u, from eq. (3.16) and the efficiencies of the BIS system; η_c, η_s, and $\eta_{24\text{-}hours}$ from eqs. (3.17), (3.18) and (3.19) respectively.

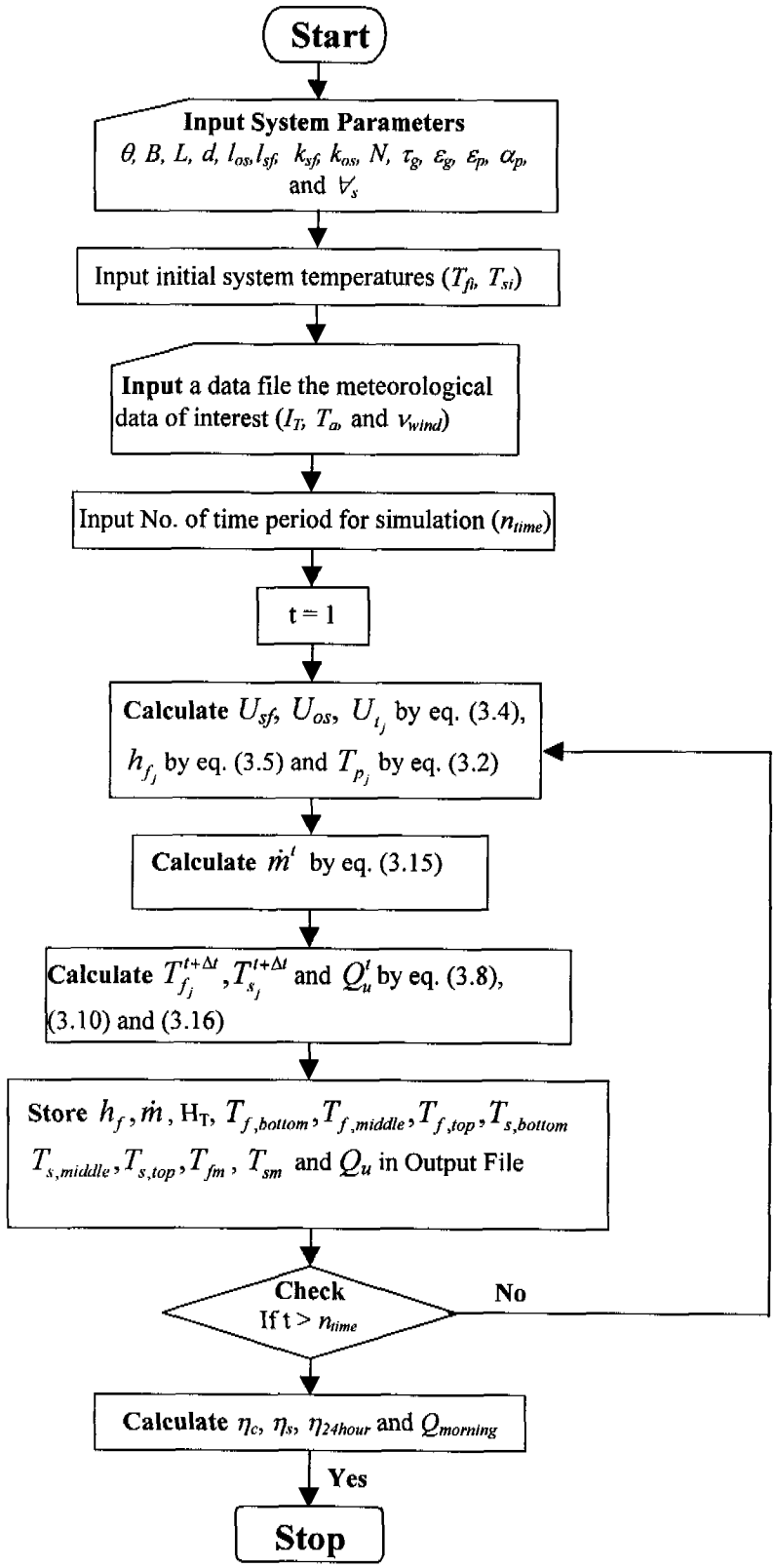

Fig. 5.1 Flow chart of simulation program

5.3 System Simulation Parameters

All simulations in this study were performed using the values of the system parameters given in Table 5.1.

Table 5.1 Parameters of the system used in the simulation.

Parameter	Value
Inclination angle of the system, θ	15° *
Latitude of test location, *Lat*	15° (north)
Collector width, B (m)	1.1 *
Collector length, L (m)	1.7 *
Average channel depth of the collector passage, d (m)	0.0425 *
Wall insulation thickness, l_{os} (m)	0.03 *
Insulated partition thickness, l_{sf} (m)	0.035 *
Wall insulation heat conductivity, k_{os} (W/mK)	0.07 **
Insulated partition heat conductivity, k_{sf} (W/mK)	0.15 **
Number of glass cover, N	1
Transmittance of glass cover, τ_g	0.88 **
Emittance of glass cover, ε_g	0.88 **
Emittance of absorber plate, ε_p	0.95 **
Absorptance of absorber plate, α_p	0.8 **
Water volume in storage tank, $\forall_s$ (liters)	273 *
Heights ($h_2 - h_1$) and ($h_3 - h_4$) in Fig. 3.4 (m)	0.10*
Heights ($h_3 - h_2$) and ($h_4 - h_1$) in Fig. 3.4 (m)	0.46*

* Obtained from measurement

** Obtained from manufacturer's specifications

5.4 Determination of Overall Flow Coefficient, K_f

5.4.1 Determination Procedure

Beside the parameter of the system given in Table 5.1, there is one more parameter, i.e. the overall flow coefficient K_f, which appears in eq. (3.15) and must be known so that the thermosyphon mass flow rate, $\dot{m}$, of the water circulating in the system can be predicted by the simulation. K_f is the overall effects of all frictions occurred along the water flowing passage throughout the system. K_f accounted for the frictions of the valve entrance and exit, the distributors, the walls in the collector channel and in the storage. It has been mentioned earlier in Chapter 3 that the average value of K_f is difficult to be theoretically determined from the physical properties and configurations of those components along the flow passage. It is suggested to determine K_f from experimental tests on the system. In the experiment, if the value of $\dot{m}$ could be measured accurately, the value of K_f would be determined directly using eq. (3.15) as other parameters in the system could be easily obtained by the measurements. Unfortunately it is not easy to measure the thermosyphon mass flow rate occurring in the constructed BIS solar water heater because the flow rate is very small.

Hence, a trial and error procedure is proposed to determine the value of K_f from the experimental data obtained from the tests on the system. Several values of K_f are guessed systematically and input to the simulation program. For each value of K_f, the program predicts the average temperature of the water in the storage tank, T_{sm}, at any time interval of interest in accordance with the given meteorological data observed from the experimental test. These simulated values of T_{sm} are compared with their corresponding values of T_{sm} observed from the experiment. Their errors are estimated and the standard errors of estimate (SEE) of T_{sm} is then calculated by

$$\text{SEE} = \left| \frac{\sqrt{\sum_{i=1}^{n} (T^t_{sm,cal_i} - T^t_{sm,\exp_i})^2}}{n-1} \right| \quad (°C) \qquad (5.1)$$

where $T^t_{sm,cal}$ = average temperature of the water in the storage resulted from simulation at any time t (°C),

$T^{t}_{sm,exp}$ = average temperature of the water in the storage resulted from experiment at any time t (°C),

n = number of the data.

Finally the value of K_f that produces the minimum value of SEE is therefore selected for the system under the considered condition.

The water in the collector channel flows upward during the heating period and, if provision for preventing reverse thermosyphon flow is not installed in the system, the water would flow downward in the collector channel during the night or cooling down period. Hence the value of the overall flow coefficient K_f during the heating may differ from that during the cooling since different friction resistances can be expected from the opposite direction of flow through any passage. Hence K_f is considered from two parts of data of each experimental test run, i.e. K_f for the heating period and K_f for the cooling period. For the heating period, K_f is suggested to determined from the days with high solar radiation intensity, say about 20 MJ/m^2. Note that with such a high insolation day it is ascertained that the water flow exists in the system with a rate high enough to give accurate results of K_f.

The value of K_f for the heating period is determined using the experimental data over the period which the thermosyphon head, H_T, calculated by eq. (3.12) is found to be positive value whereas K_f for the cooling period is determined from the period when the thermosyphon head is negative. As, in each test, the system cooling down period occurred in the evening after the daytime heating up period, K_f for the heating period is determined first and then the accepted value of K_f for the heating period will be used to determine K_f for the cooling period.

For each value of K_f, the step of the determination can be described as the following.

(a) Procure the input file of the meteorological data of the day that has the total solar radiation about 20 MJ/m^2.

(b) Assume an initial value of K_f, generally $K_f = 0$ is used, and then put in the simulation program.

(c) Run the program to simulate $T^t_{sm,cal}$ at any time t.

(d) Compare $T^t_{sm,cal}$ with its corresponding $T^t_{sm,\exp}$ extracted from the stored output file and calculate SEE of T_{sm} using eq. (5.1).

(e) Change the value of K_f and repeat steps (c) to (d).

(f) Comparing the values of SEE of T_{sm} obtained from various values of K_f, choose the value of K_f that gives the minimum value of SEE of T_{sm}.

5.4.2 Determination Results

In Chapter 4, the developed built-in-storage solar water heating system were tested for 24 hours starting from early morning at 06.00 hours under 3 cases of different operations of the check-valve installed in the flow passage. It is found appropriate to mention the three cases again as the following.

Case 1: The check-valve in the flow passage was forced open throughout the test i.e. reverse circulation may occur at night.

Case 2: The check-valve was allowed to work freely throughout the test. The valve opening is dependent on the pressure difference between each side of the valve lid.

Case 3: The check-valve was allowed to work freely during the day but forced close at night i.e. no reverse circulation at night may occur.

The best values of K_f obtained using the above mentioned determination procedure for both heating and cooling periods of several experimental test runs are shown in Table 5.2. For purpose of sample illustration of how the best value of K_f is selected, the plot of several values of K_f obtained for Case 2 on 15/11/2002 are presented in Fig 5.2. It is clearly seen that, for heating case, the minimum value of SEE of 0.08 °C (or about 0.2 % of the average value of T_{sm} of 40.0 °C) is found at K_f = 0.00045 $kg.s^{-1}.(mK)^{-1/2}$. Similarly, in the cooling period case, the value of SEE is minimum when K_f = -0.0002 $kg.s^{-1}.(mK)^{-1/2}$. Note that the negative K_f means that the flow is in the reverse direction. The SEE is about 0.02 °C (or 0.05 % of the average value of T_{sm} = 42.4 °C) during the cooling period. In other cases, similar trends were found as given in Appendix B.

In Table 5.2, it is found that K_f for heating period of Case 1 is higher than those of Case 2 and Case 3. As K_f is directly related with the mass flow rate of water circulating in

the system, this mean that the flow rate in Case 1 was higher than the other two cases. Note that with higher K_f, the resistance to flow is less resulting in higher flow rate. This can be explained by the fact that, in Case 1, the check-valve installed in the flow passage was forced to fully open throughout the day (and the night as well). The resistance to flow was therefore less than those of the other two cases in which the check-valve was allowed to work freely, i.e. the valve was usually partly opened depending on the driving forced created by differential pressures of water located at both sides of the valve. The valve was then very rare in the full opening position. Similar results were also found in the case of cooling at night in which relatively very high reverse flow was shown in Case 1 in comparison with those in the other two cases.

Note that, in Case 3 in which the check-valve was forced close, the value of K_f obtained from the night was not zero as it must be in reality. However the obtained value was very small and actually very close to zero. The small discrepancy may be explained by the errors in experimental measurements. It should also be noted here that the value of K_f for night-time period was found quite low for Case 2 indicating that the installed check-valve could significantly stop the reverse circulation.

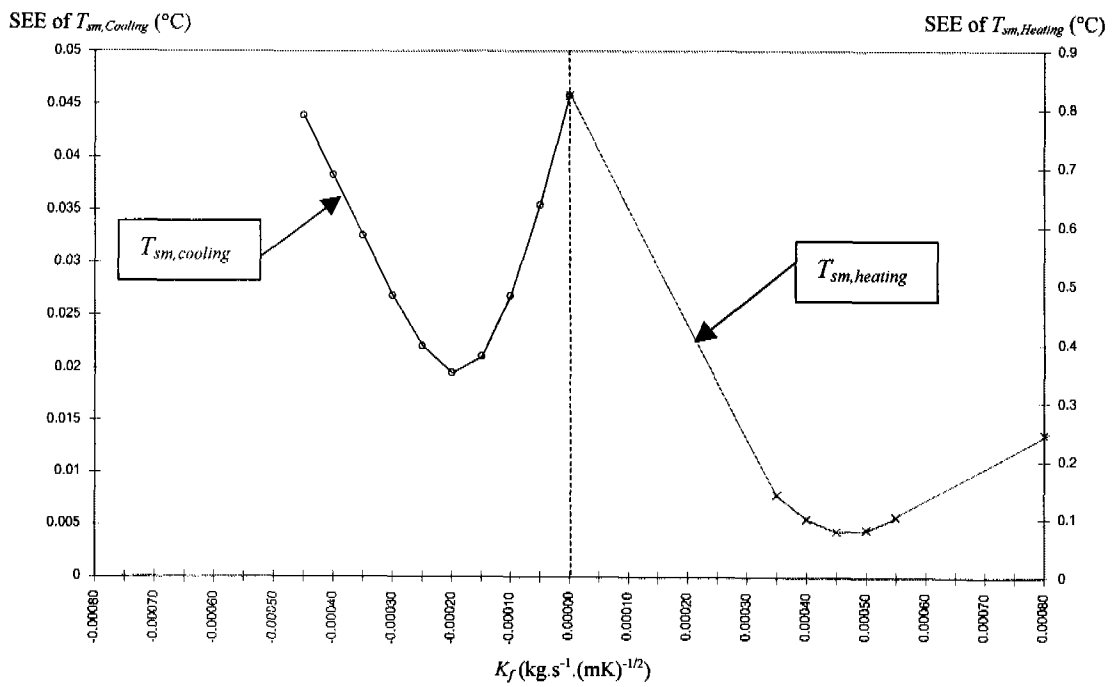

Fig. 5.2 Standard errors of estimate of T_{sm} found at different values of K_f.

Table 5.2 Best values of the overall flow coefficient K_f obtained for three different operations of check-valve.

Operation of check-valve	Date of Experiment	I_T (MJ/m^2)	Heating Period		Cooling Period	
			Value of K_f (kg.s^{-1}.(mK)$^{-1/2}$)	SEE (°C)	Value of K_f (kg.s^{-1}.(mK)$^{-1/2}$)	SEE (°C)
Case 1: check-valve open throughout the test (reverse circulation at night)	9/10/2002	20.7	0.00150	0.18	-0.01550	0.10
Case 2: check-valve operated freely throughout the test	15/11/2002	20.7	0.00045	0.07	-0.00020	0.02
Case 3: check-valve operated freely during the day but closed at night (no reverse circulation at night)	12/7/2002	19.7	0.00060	0.08	-0.00025	0.15

5.5 Simulation Results and Discussion

To validate the developed mathematical model in predicting the system performance under Case 2 which is the normal condition of check-valve in actual operation, the thermal performance parameters of the system such as T_{sm}, T_{fm}, η_c, η_s, η_{24hour} and $Q_{morning}$, simulated by the program described in section 5.2 were compare with those obtained from the experiments. The meteorological data, i.e. I_T, T_a, V_{wind}, recorded from several test runs presented in Chapter 4 under Case 2 were used as the inputs to the program along with the fixed system parameters given in Table 5.1. The values of overall flow coefficients K_f (for heating and cooling period) for Case 2 of check-valve operation shown in Table 5.2 were then taken for the simulation. A sample of the simulation results obtained for the test on the system under Case 2 on 15/11/2002 is shown in Fig.5.3.

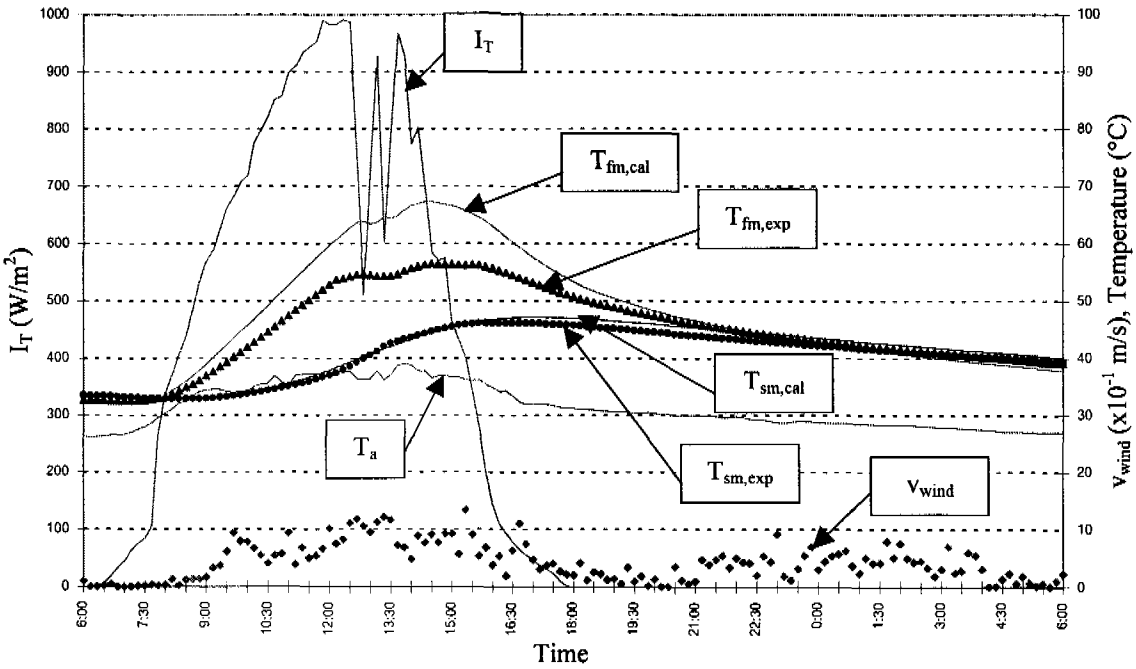

Fig.5.3 Simulation results in comparison with experimental results on 15/11/2002

It can be seen from the figure that there is a quite good agreement between the values of $T_{sm,cal}$ obtained from the simulation and the values of $T_{sm,exp}$ observed from the experiment. The average deviation (i.e. the value of SEE) is about 0.03 °C or 0.07 % of the average value of T_{sm} of 40.6 °C throughout the test period. The simulation results obtained from other test runs are similarly illustrated and given in Appendix C. Their corresponding values of SEE between $T_{sm,cal}$ and $T_{sm,exp}$ are provided in Table 5.3. The results show that the model is able to simulate the mean storage temperatures of the system in agreement with the experiment values. The maximum SEE found is about 0.12 °C on 11/10/2002.

In Fig. 5.3, too high values of $T_{fm,cal}$ estimated by the model can be seen during the heating period. The over estimations of $T_{fm,cal}$ may come from several factors. The property deteriorations of the collector components, such as glass cover, absorber plat and insulation, after several test runs might result in lower performance than that estimated by the simulation using their original properties taken from the manufacturers' specifications. The errors in estimating the overall flow coefficient K_f from the experimental data may also contribute some errors in determining the thermosyphon flow rate in the system which effects the prediction of $T_{fm,cal}$. Detailed investigations on these effects to improve the accuracy in simulating the value of T_{fm} should be carried out.

However, all parameters for characterizing the thermal performance of the system in this study; those are η_c, η_s, η_{24hour} and $Q_{morning}$, are calculated using the temperature of water in the storage, T_{sm}, not that of water in the collector channel T_{fm}. Hence the developed model can be used to determine these system performance parameters with confidence. This can be confirmed by Table 5.3 which illustrates the simulated results of these parameters obtained from several test runs in comparison with those observed from the experiments. The percentage errors for all parameters in most test runs are found to be within ± 12 % except the test run under very low solar radiation (i.e. 17/8/2002).

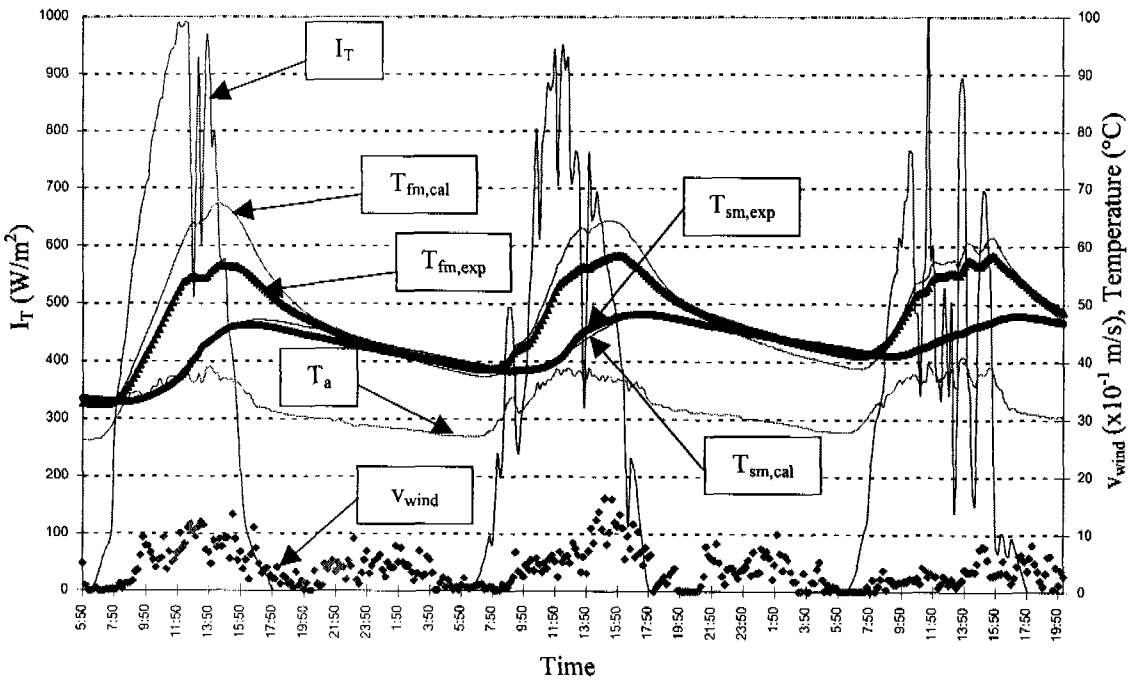

Fig. 5.4 Simulation results of three-consecutive-day in comparison with those obtained from experiments.

Figure 5.4 illustrates the ability of the developed model in simulating the dynamic variations of system temperatures in response to the changes in solar irradiance, ambient temperature and wind velocity for three consecutive days. The system temperatures measured from the experiment conducted during these three days are also presented for comparison. Satisfactory agreement is shown in the prediction of the mean storage temperatures of the system, T_{sm}. But, for the values of the mean temperature of the water inside the collector channel, T_{fm}, although large deviations are found during the heating period, especially on sunny days, the simulated values vary following the trends observed from the experiment. However, as mentioned earlier, T_{fm}, does not affect the prediction of

the performance of the system. It can be concluded here that the developed model can be used to determine the long-term performance of the BIS system if the long-term meteorological data are available.

Table 5.3 Thermal performances of the BIS system resulting from simulation and experiment when check-valve operated freely through the test.

Date	I_T (MJ/m²)	$\overline{T}_{sm}$ (°C)	SEE (°C)	η_c (%)		% error	η_s (%)		% error	η_{24hour} (%)		% error	$Q_{morning}$ (MJ)		% error
				Cal	Exp		Cal	Exp		Cal	Exp		Cal	Exp	
17/8/2002	11.2	31.1	0.10	34.8	43.3	-19.6	65.8	60.4	8.9	16.0	17.9	-10.6	8.9	9.3	-4.3
3/10/2002	20.7	41.2	0.10	38.8	39.9	-2.7	64.1	61.7	3.9	19.7	18.7	5.3	14.7	14.2	3.5
11/10/2002	25.2	41.9	0.12	36.2	37.1	-2.4	62.7	63.3	-0.9	16.4	16.7	-1.8	19.0	19.0	0
13/11/2002	18.7	38.3	0.10	38.9	36.1	7.7	63.8	60.7	5.1	19.2	17.5	9.7	14.6	13.1	11.4
15/11/2002	20.7	40.6	0.03	38.3	38.2	0.2	61.7	61.5	0.3	18.2	16.4	11.0	15.0	14.2	5.6

Note: $\overline{T}_{sm}$ = average value of the mean storage temperature, T_{sm}, throughout the experimental test

SEE = standard error of estimate of T_{sm}

% error = (Cal – Exp) / Exp x 100

η_c = daytime collecting efficiency

η_s = storage efficiency during the cool down period at night

η_{24hour} = system efficiency during 24 hours

$Q_{morning}$ = amount of energy stored in the storage tank before sunrise of the next morning